THE INFLUENCE OF SUPPORT RIGIDITY ON WATERHAMMER PRESSURES AND PIPE STRESSES

A.G.T.J. Heinsbroek

Industrial Technology Division
DELFT HYDRAULICS
P.O. Box 177, 2600 MH Delft
The Netherlands

A.S. Tijsseling

Department of Civil Engineering
University of Dundee
Dundee DD1 4HN, Scotland
United Kingdom

Abstract

It is well known that the support conditions may have a significant influence on the waterhammer behaviour of liquid-filled pipe systems. For rigidly supported systems, classical waterhammer calculations generally give reliable predictions of the extreme pressures and stresses in the system. For more flexibly supported systems, classical predictions may fail due to the dynamic interactions between the vibrations of liquid and pipes. Fluid-structure interaction (FSI) effects must then be taken into account.

In the present paper two items are investigated as a function of the rigidity of pipe supports: i) the validity of conventional waterhammer analyses and ii) the magnitudes of the extreme pressures and stresses.

Calculated results show that in the test case considered conventional waterhammer analyses fail when the rigidity of bend supports is less than the axial stiffness of one metre of pipe. Maximum stresses appear to be higher in the more flexible pipe systems, but the forces acting on the supports are lower.

1. Introduction

The *classical theory of waterhammer* [Chaudhry 1979; Wylie & Streeter 1993] describes the transient behaviour of liquid contained in pipe systems in terms of dynamic pressures and velocities. The elasticity of the pipes is taken into account, but their inertia and motion in longitudinal (axial) direction is completely disregarded. The stresses in the pipe follow quasi-statically the pressure P in the liquid. The hoop stress σ_h is

$$\sigma_h = \frac{R}{e} P \tag{1}$$

and the axial stress σ_{ax} is

$$\sigma_{ax} = 0 \quad \text{or} \quad \sigma_{ax} = \nu \frac{R}{e} P \quad \text{or} \quad \sigma_{ax} = \frac{1}{2} \frac{R}{e} P \tag{2}$$

depending on the support conditions of the pipe under consideration; R/e is the ratio of inner pipe radius to wall thickness and ν is Poisson's ratio. Anchor forces are estimated from the dynamic pressures [van der Weijde 1985].

The *extended theory of waterhammer* [Skalak 1956; Wiggert et al. 1985] requires a full stress analysis of the pipe system since i) the dynamic axial pipe stress (or displacement) is a variable in the extended waterhammer equations and ii) the axial vibrations of dead ends, elbows and T-pieces generate waterhammer in the liquid. All liquid-pipe interaction mechanisms [Tijsseling & Lavooij 1990] are taken into account and, in addition to the liquid pressures and velocities, dynamic pipe stresses and displacements are calculated. Anchor forces are derived from the dynamic stresses [Bürmann & Thielen 1988]. An extensive review of literature dealing with liquid-pipe interaction is given in [Tijsseling 1993].

It is believed that the classical theory is valid as long as the pipe system is sufficiently rigidly anchored. It is known, however, that severe deviations (changed amplitudes and frequencies) from classical predictions may occur when essential parts of the system are not rigidly anchored [Wood 1969; Hatfield et al. 1982]. The extended waterhammer theory should then be applied.

Entirely rigid pipe supports or anchors do not exist. The aim of this paper is to investigate the influence of pipe support rigidity on waterhammer calculations. The supports are considered rigid if classical waterhammer calculations are valid. The validity is approved when classically calculated results agree well with results calculated with extended waterhammer theory. It is still up to the engineer what he/she regards as acceptable in this respect. Furthermore, the extreme pressures and stresses occurring in a transient event are studied as a function of pipe support rigidity. This study relates to the question whether a pipe system should be fairly rigid or whether it should be more flexible in coping with waterhammer loads. Cost aspects play a role since support devices, like snubbers, can be expensive.

One test problem, a reservoir-pipeline-valve system, is analysed numerically. The pipeline contains six bends, which are supported by linear springs. The stiffness of the springs is varied from entirely rigid to entirely slack. The response of the system to very rapid valve closures is investigated.

2. Test problem

The significant effect of pipe motion on contained liquid behaviour has been observed in many pipe systems, e.g. [Blade et al. 1962; Swaffield 1968-1969; Wood & Chao 1971; Krause et al. 1977; Kellner et al. 1983; Wiggert et al. 1985; Vardy & Fan 1989; Kruisbrink & Heinsbroek 1992]. A more complete survey can be found in [Tijsseling 1993]. Most of the pipe systems studied were relatively small and partly unsupported; some of them were even suspended by wires to take away any resistance to pipe motion. Problems with apparently rigid supports not being entirely rigid occurred [Swaffield 1968-1969; Wilkinson 1980, p. 197].

The largest laboratory system is that of [Kruisbrink & Heinsbroek 1992] and it is this particular system that is analysed herein. Seven straight steel pipes (109 mm inner diameter, 3 mm wall thickness) connected by six 90-degrees mitre bends form the three-dimensional pipe system schematically shown in figure 1. The total length of the system is 77.5 m. It is supported by long thin steel cables and bearings at two bends (B and G), thus allowing for significant longitudinal, flexural and torsional deformations. The anchors at the ends A and B have a measured axial stiffness of 317 kN/mm and 214 kN/mm, respectively. Water is flowing from a constant head air-vessel at one end of the pipe system to a valve at the other end. Severe transients were generated by the nearly instantaneous (within 10 ms) closure of the valve. The pressure in the system is

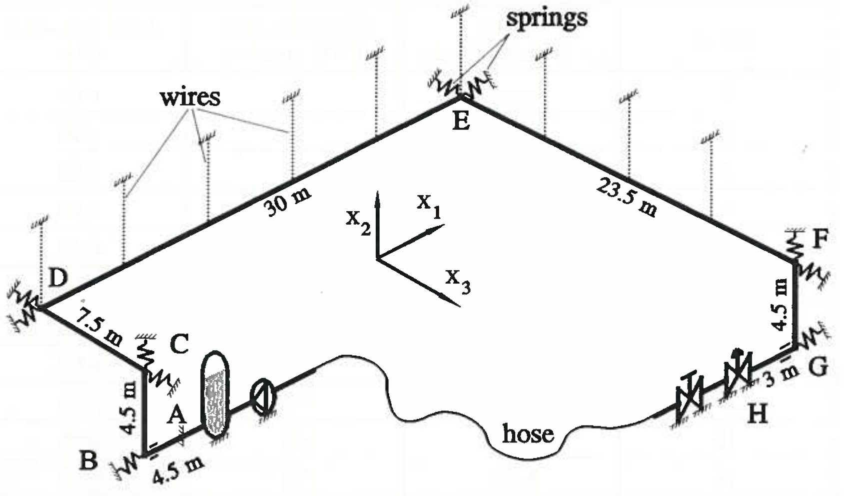

Figure 1. Schematic representation of pipe system analysed.

taken sufficiently high to prevent cavitation.

The pipe system was designed and constructed to validate a numerical model for fluid-structure interaction (FSI). To this end the system was deliberately made very flexible, so that FSI effects are predominant. Whereas for rigidly supported pipe systems the classical waterhammer theory is adequate (e.g. [Simpson 1986]), an analysis of the very flexible system at issue requires extended waterhammer theory [Kruisbrink & Heinsbroek 1992].

In practice most pipe systems are neither entirely rigid nor very flexible. To assess the transient behaviour of pipe systems of intermediate rigidity, the system of figure 1 is analysed numerically for different degrees of rigidity. All bends are held by 10 linear springs (figure 1), the stiffness of which is varied from infinitely large (in the classical case) to zero (table 1). The spring stiffnesses in table 1 are relative to the axial stiffness EA_t/L of $L = 1$ m of pipe, which is 215.6 kN/mm. The cross-sectional pipe-wall area A_t is 1078 mm^2 and Young's modulus E of the pipe's steel is 200 GN/m^2. The latter value was provided by the manufacturer, just as Poisson's ratio ν being 0.3 and the steel's mass density ρ_t being 8000 kg/m^3. The stiffness of the suspension wires is 0.285 kN/mm in the vertical direction and 0.000243 kN/mm in the horizontal direction. The properties of water at 20 °C are obtained from tables in literature: the mass density ρ_f is 998.2 kg/m^3 and the bulk modulus K_f is 2.19 GN/m^2. The test case considered here is with a 5.87 bar gauge pressure in the air-vessel and an initial flow velocity of 0.3 m/s. The (American) Darcy-Weisbach friction coefficient f [Wylie & Streeter 1993, p. 21], including local losses, is measured 0.031.

Run #	*Rigidity* (∗ 215.6 kN/mm)	*Simulation time* (CPU minutes)	*Main frequency* (Hz)
1	classical	19	4.05
2	1000	56	4.08
3	100	56	4.08
4	10	57	4.08
5	1	72	4.08
6	0.1	89	4.05
7	0.02	96	4.00
8	0.01	96	4.00
9	0.005	96	3.93
10	0.002	96	3.75
11	0.001	98	3.35
12	0.0006	98	3.02
13	0.0005	99	2.89
14	0.0004	100	2.82
15	0.00036	99	2.79 / 5.75
16	0.0003	100	5.61
17	0.0002	100	5.35
18	0.0001	99	5.20
19	0.00001	98	5.09
20	0.000001	98	5.05
21	0	98	5.02

Table 1. Numerical simulations performed.
Rigidity of all bend supports relative to axial rigidity of one metre of pipe.
Simulation time on a 486-33 PC
(depends on the number of fluid-structure iterations needed).
Main frequency in calculated pressure histories.

3. Numerical simulation

Numerical simulations were carried out with the FLUSTRIN software owned by DELFT HYDRAULICS [Lavooij & Tijsseling 1989; Kruisbrink & Heinsbroek 1992]. The software has been validated against physical experiments known from literature and against numerical results of other investigators. It is based on extended waterhammer theory for the liquid and extended beam theory for the pipes. Fluid-structure interaction (FSI) mechanisms due to i) the motion of anchors and bends (junction coupling), ii) the coupled radial and axial motion of the pipe walls (Poisson coupling), and iii) the mutual friction between liquid and pipes (friction coupling), are taken into account. The software is valid for long-wavelength acoustic phenomena, cavitation is assumed not to occur and the displacements of the pipes must be within the range of linear elasticity.

The transient behaviour of the pipe system in figure 1 has been simulated with FLUSTRIN, using the data provided in the previous section as input. It is repeated here that the suspension wires are modelled as linear springs with both vertical and horizontal gravity components, that the air-vessel has a constant pressure and that the valve closure is almost instantaneous. The anchors at A and H are considered to be entirely rigid. At B and G displacements in the X_2- and the X_3-direction are fully restrained as well as rotations about these two axes. The rigidity of all linear springs at the bends B, C, D, E, F and G is stepwise decreased by the same amount from entirely rigid to entirely slack, as indicated in table 1. Hence, one classical waterhammer calculation (no pipe motion) and 20 FSI calculations were carried out. In the numerical calculation the pipe was divided into 51 elements which corresponds to a numerical time step of 1.2 ms.

4. Calculated results

Waterhammer pressures

Pressure histories calculated close to the valve are shown in figure 2 for six different rigidities of the bend supports. The classical pressure history, which is based on a calculation ignoring any axial pipe stresses, is shown as a reference. The main frequency of the classical waterhammer wave is 4.05 Hz ($c_f/(4L)$ with c_f = 1257 m/s and $4L$ = 310 m) and its amplitude is about 3.76 bar (Joukowsky: $\Delta P = \rho_f c_f \Delta V$ with ρ_f = 998.2 kg/m^3 and ΔV = 0.3 m/s).

The axial motion of bends is negligible when the rigidity of their supports is 1000 times larger than the axial stiffness of one metre of pipe. In that case junction coupling, which is the most important FSI-mechanism, does not exist. Consequently, the first $4L/c_f$ = 0.25 seconds of the pressure histories calculated with extended and classical theory are nearly the same (figure 2, upper left frame). Later on the differences become bigger due to cumulative Poisson coupling effects. In particular, pressure peaks of increasing magnitude occur after each time interval of $2L/c_f$ seconds. A similar phenomenon has been predicted for a straight pipe by Wiggert et al. [1986] and Tijsseling & Lavooij [1989], but its physical importance may be questioned since the phenomenon has, as far as the authors know, never been observed in practice.

The calculated pressure histories for bend supports with a rigidity equal to that of one metre of pipe (figure 2, upper right frame) resemble those obtained for a thousand times larger rigidity. Therefore, the supports can still be regarded as rigid. When their rigidity becomes lower, calculated pressure histories will differ from the two shown in the two upper frames of figure 2.

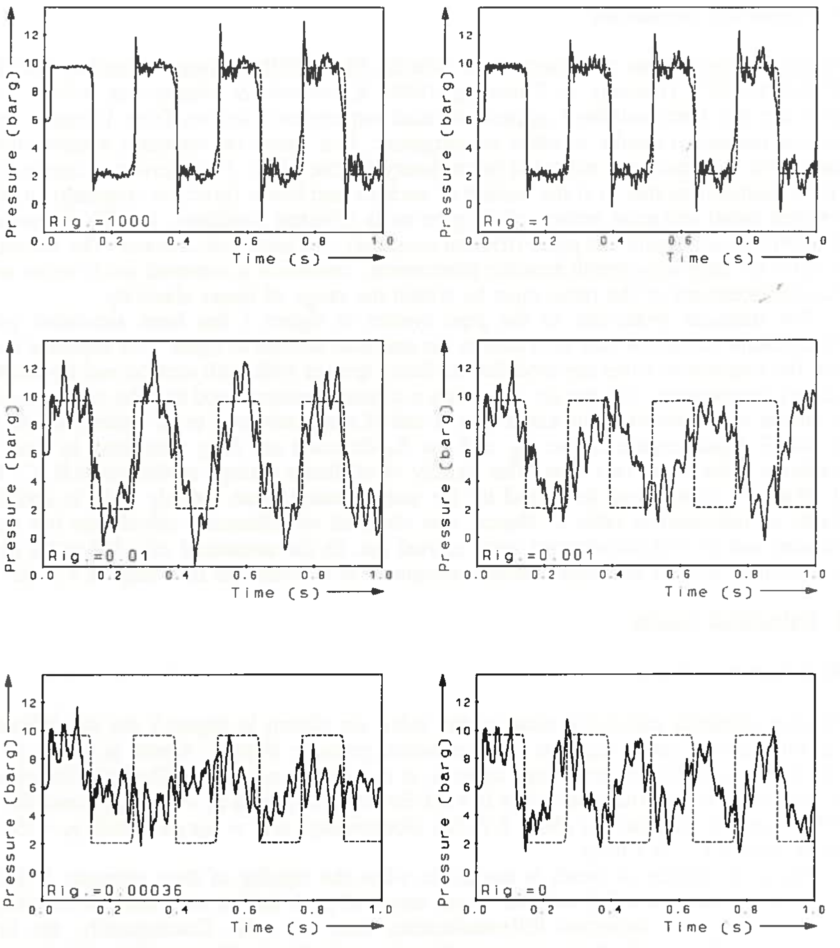

Figure 2. Pressure histories at valve for six different rigidities of the bend supports. (—— extended waterhammer theory, - - - classical waterhammer theory)

When the bend support rigidities are 100 times lower than the axial stiffness of one metre of pipe, which is still large compared to the horizontal stiffness of the suspension wires, the pressure close to the valve as calculated with extended waterhammer theory is completely different from the one calculated with classical theory (figure 2, middle left frame). A frequency of 29 Hz, superimposed on the basic frequency of 4 Hz, can be discerned and the whole signal becomes more triangular as opposed to the rectangular shape of the classical signal. The pressure peaks substantially (up to 100%) exceed the classical Joukowsky pressure. With the steady-state pressure equal to nearly 6 barg (as is the case in all simulations considered) some cavitation would occur in reality, but it is neglected here.

Further decreasing the rigidity by a factor of 10 (figure 2, middle right frame) leads to a shift of the pressure wave's main frequency from 4 Hz towards 3 Hz. This frequency is considerably lower than the classical one.

When the rigidity is further decreased to a value of 0.00036, the pressure signal develops a somewhat chaotic character (figure 2, bottom left frame). It is not easy to distinguish the basic frequency in this case. The authors have based their assessment of two frequencies (2.79 Hz and 5.75 Hz in table 1) on a simulated time interval of 4 seconds (not shown here).

A qualitatively similar pressure signal, as with rigidity 0.001, is calculated when all bend supports are removed (figure 2, bottom right frame). Now, however, the main frequency of the pressure wave is considerably larger than the classical one. This larger frequency, the trident shape just after valve closure and the triangular shape later on, are confirmed by physical experiment [Kruisbrink & Heinsbroek 1992].

The frequency shift in the pressure waves as caused by FSI mechanisms is studied in figure 3. Based on the values given in table 1, the lowest frequency in the pressure signals is portrayed as a function of the rigidity of the bend supports. For bend support rigidities larger than one per cent of the axial stiffness of one metre of pipe, the main pressure wave frequency is very close to the 4.05 Hz found with classical theory. For rigidities smaller than 10^{-5} times the axial stiffness of one metre of pipe, the frequency is close to the 5.02 Hz predicted and observed in a system without bend supports. A transition area exists for rigidities between 10^{-5} and 10^{-2}, with more or less chaotic behaviour when the rigidity is between 0.0003 and 0.0006. The "chaos" is most severe for rigidity 0.00036 (figure 2, bottom left frame). It is noted that all frequencies in table 1 were assessed by finding the best fit of a sine wave through the pressure histories at four different locations. Since we are only interested in the lowest frequency, this method is sufficient. A Fourier analysis is required if one is also interested in higher frequencies.

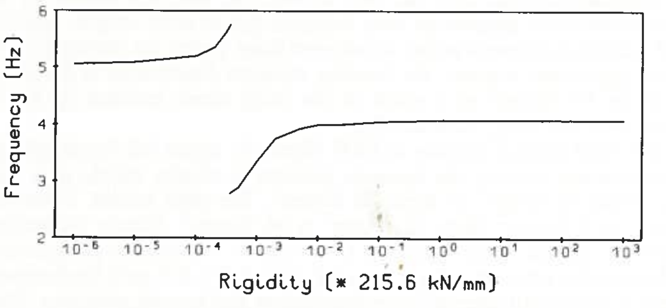

Figure 3. Main frequency of pressure wave versus rigidity of bend supports (see table 1).

Pipe stresses

The ANSI/ASME B31 Codes for pressure piping recommend application of the equivalent stress according to Tresca at the outer fibre of the pipe wall [Helguero 1985]. The radial stresses are assumed to be zero, indicating a plane-stress case. The principal stresses expressed in terms of the total axial stress σ_{tax} (resulting from axial forces and bending moments), the total shear stress τ_{ts} (resulting from shear forces and torsional moments) [Heinsbroek 1993] and the hoop stress σ_h are [Gere & Timoshenko 1987]:

$$\sigma_1 = \frac{1}{2}\left[\sigma_{tax} + \sigma_h + \sqrt{4\tau_{ts}^2 + (\sigma_{tax} - \sigma_h)^2}\right] \tag{3}$$

$$\sigma_2 = \frac{1}{2}\left[\sigma_{tax} + \sigma_h - \sqrt{4\tau_{ts}^2 + (\sigma_{tax} - \sigma_h)^2}\right] \tag{4}$$

$$\sigma_3 = 0 \tag{5}$$

The convention is to sort these three stresses such that $\sigma_1 > \sigma_2 > \sigma_3$.

For a general tri-axial stress state it is assumed that yielding of the material occurs when the local stress reaches a critical value: the allowable stress σ_a. The yield condition applied here is the Tresca condition, which is preferred by the ANSI/ASME B31 Code above the Von Mises condition. The Tresca condition (equivalent stress) is defined as:

$$\sigma_e = 2\tau_{max} = \max(\sigma_1, \sigma_2, \sigma_3) - \min(\sigma_1, \sigma_2, \sigma_3) \tag{6}$$

To avoid yielding: $\sigma_e < \sigma_a$.

In the classical waterhammer theory the bending, shear and torsion of pipes is disregarded. In that case the Tresca stress σ_e equals $R/e \mid P \mid$, which follows directly from the equations (1) to (6).

The distributions of the maximum equivalent stresses according to Tresca for four cases with different rigidities are shown in figure 4. The static Tresca stress distribution, caused by dead weight and stationary flow only, is included as well (dashed line). The peaks, at positions 22.5 m, 28.5 m, 34.5 m, 40.5 m, etc., are caused by the negative bending moments at the suspension wire locations due to dead weight. The zero-moment points and maximum-moment points in between these peaks can clearly be distinguished. In the static equivalent stresses, the bending moment distribution is lifted upward by a value of about 10 N/mm^2 as a result of the hoop stress induced by the steady-state pressure of 5.42-5.87 barg (formula (1)).

When the bend support rigidity is 1000 (figure 4, upper left frame) the contribution of the waterhammer load to the dynamic solution is clearly visible as a "bottom level rise" from about 10 N/mm^2 to about 20 N/mm^2. The peak values, however, only rise with about 2 or 3 N/mm^2 from 32 N/mm^2 to 34 N/mm^2. Simply increasing the static Tresca stresses by the hoop stress σ_h ($= R/e\,\Delta P = 7$ N/mm^2) associated with the classical Joukowsky pressure ΔP ($= \rho_f c_f \Delta V$ with $\Delta V = 0.3$ m/s) inadvertently neglects the changes in the overall internal force distribution and support reactions. Therefore, the quasi-static Tresca stresses should be determined in a static pipe stress analysis by increasing the steady-state pressure distribution by the Joukowsky pressure ΔP. An alternative approach is increasing the steady-state pressure distribution by twice the Joukowsky pressure to take so into account a dynamic load factor (DLF) of 2, which is

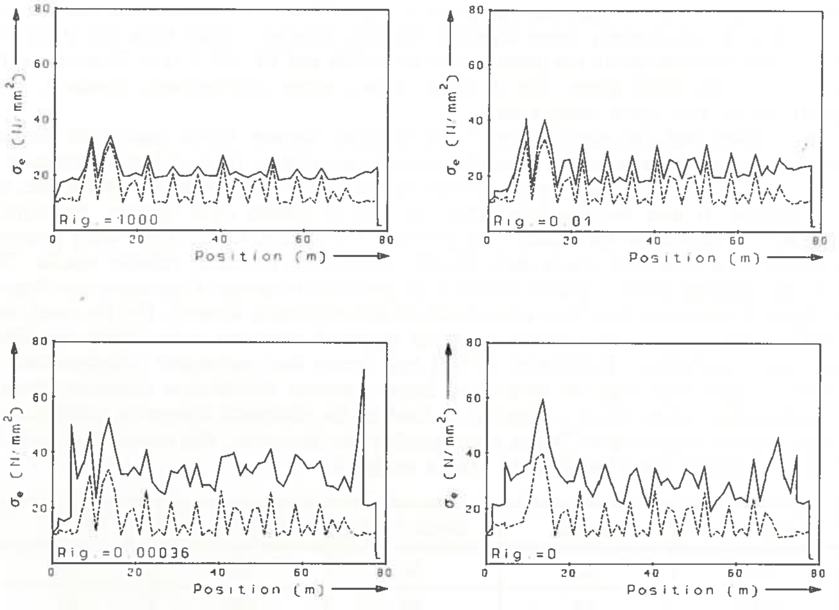

Figure 4. Distribution along the pipe system of the maximum equivalent stresses. (—— static + dynamic (FSI) solution, - - - static (steady-state) solution)

commonly used for step loads [Biggs 1963]. The results of these different methods of calculation are given in table 2, together with the results of full FSI computations.

The static + dynamic Tresca stress distribution in case of a spring support rigidity of 0.01 (figure 4, upper right frame) shows a "bottom level rise" of about the same magnitude as in the previous case, although the peaks reveal a larger increase.

When the rigidity is 0.00036 (figure 4, bottom left frame) the static + dynamic Tresca stress distribution is by no means similar in form to the static distribution and much more capricious. Upstream of elbow G (position 74.5 m) a large peak develops.

With a rigidity of 0 the distribution again changes rather drastically (figure 4, bottom right frame), be it somewhat more similar in form to the static distribution. Here a stress peak develops at mid-span of pipe CD. The increases in the Tresca stresses are substantially larger than the Joukowsky hoop stress ($R/e\ \Delta P$ = 7 N/mm^2).

It is striking to observe that the static Tresca stress distributions in the cases with support rigidity other than zero hardly show any variation. Only the peak values vary slightly (table 2, second column). The spring stiffness corresponding to a rigidity 0.00036 is 0.078 kN/mm, which is not regarded as high. The conclusion may be drawn here that as long as the bends are more or less "kept in place" the variation of the static Tresca stress distribution is insignificant. The main effect of releasing the springs is that elbows C and F are enabled to rotate about the X_1-axis, thus relieving the rotational spring stiffness supporting the upstream end point of pipe CD and the downstream end point of pipe EF with consequently lower clamping bending moments. Apart from this effect, the static stress distribution in the unrestrained pipes DE and EF (16.5 m to 70 m) is nearly identical to the other three. The dynamic Tresca stress distributions, however, vary greatly in the four cases considered.

It is noted that the contribution of the dynamic stresses to the equivalent stresses becomes proportionally larger when the initial flow velocity (here 0.3 m/s) increases.

In table 2 the maximum Tresca stresses following from the different approaches are summarised. It may be concluded that, in case of almost rigid springs, the simple approach of increasing the steady-state pressure distribution by the Joukowsky pressure followed by a structural steady-state (static) computation produces reliable results. The Poisson coupling effects, clearly visible in the pressure histories of the upper two frames of figure 2, appear to be of less importance for the maximum stresses. For the cases with spring stiffnesses less than almost rigid this approach turns out to be highly unreliable and non-conservative. Heinsbroek [1993] has shown that uncoupled computations, in which at each time step the temporary liquid pressure distribution (resulting from a waterhammer computation) is applied as load in the structural dynamics computation, lead to far too conservative Tresca stress predictions. However, this conclusion might be highly dependent upon the pipeline system analysed.

Rigidity	Static	Static+ΔP	Static+$2\Delta P$	FSI
1000	32	34	36	34
0.01	33	36	40	41
0.00036	34	37	40	70
0	40	43	46	60

Table 2. Maximum equivalent (Tresca) stresses in N/mm^2 for four different rigidities of the bend supports and different methods of calculation (ΔP = classical Joukowsky pressure load).

Table 3 gives the maximum values of the pressures, stresses and reaction forces occurring in the pipeline system during one second of simulation. The maximum pressures in the rigid pipe systems (rigidity 1 - 1000) are much higher than the 9.63 barg predicted by classical waterhammer theory (if friction effects are disregarded: static pressure of 5.87 barg at valve + dynamic Joukowsky pressure of 3.76 bar). This is due to the pressure peaks of increasing magnitude (see figure 2, top frames), which are believed to be physically unrealistic. From rigidity 0.002 on, the maximum pressure decreases when the system becomes more flexible. The maximum stresses, however, do not decrease. They are the lowest in the most rigid systems. On the other hand, the forces on bearings, anchors, and, in particular, the bend supports, are the highest in the rigid systems. The forces in the suspension wires are the highest in the more flexible systems, where the vertical junction force components at bends C and F are no longer directly borne by the vertical bend supports. The vertical junction force components are thus no longer restrained to excite the system in vertical direction, with consequently larger amplitudes of the suspension wire forces.

Rigidity (* 215.6 kN/mm)	Tresca stress (N/mm^2)	Anchor / bearing force (N)	Bend support force (N)	Suspension wire force (N)	Pressure (barg)
1000	34	5658	6219	1173	12.94
100	34	5674	6273	1173	12.92
10	34	5688	6129	1176	13.25
1	35	5324	5885	1177	12.30
0.1	38	4974	4732	1197	12.00
0.02	41	5039	3193	1234	13.17
0.01	41	5047	2548	1345	13.32
0.005	40	5050	1959	1405	12.18
0.002	42	5052	1774	1412	12.60
0.001	44	5053	1683	1488	12.45
0.0006	52	5052	1247	1480	12.05
0.0005	58	5052	1093	1520	11.91
0.0004	66	5051	1000	1595	11.75
0.00036	70	5051	951	1575	11.67
0.0003	65	5051	863	1555	11.56
0.0002	63	5049	673	1564	11.35
0.0001	52	5045	409	1555	11.10
0.00001	59	5022	84	1548	10.87
0.000001	59	5011	12	1543	10.84
0	60	5009	0	1543	10.84

Table 3. Maximum values of the Tresca stresses, forces on anchors (A and H) and bearings (B and G), forces on bend supports, forces on suspension wires, and fluid pressures, as a function of the rigidity of the bend supports.

5. Discussion

It is known that the classical waterhammer theory is adequate for either very rigid or very heavy pipe systems. The classical theory fails when the pipe system has a certain amount of flexibility and the valve closure is rather rapid. These matters are confirmed by the pressure histories in figure 2. The behaviour of the main pressure wave frequency as a function of bend support rigidity is most interesting (figure 3). A nearly discontinuous transition from a low frequency for larger rigidities to a high frequency for smaller rigidities seems to occur in the vicinity of rigidity 0.00036. The pressure history at the valve is whimsical in that case (figure 2, bottom left frame). One might question whether pipe supports with a rigidity of (0.00036 * 215.6 =) 0.078 kN/mm are found in 4" (schedule 10 S) pipe systems in practice. Pipe clamps connected via a bar to wall or floor are not uncommon and their rigidity can be very low. Unsupported bends have no rigidity at all.

To have a physical reference frame, the rigidity of the bend supports has been quoted relative to the axial stiffness of one metre of pipe. This one metre is quite arbitrary. It has been chosen for lack of a better length scale. The authors did not want to use a length scale based on static considerations for the strongly dynamic problem treated herein. A possible dynamic length scale is: $c_s T_{cef}$ with c_s the speed of propagation of axial stress waves and T_{cef} (>0) the effective closure time of the valve (defining the steepness of the wave fronts). In the test problem analysed $c_s = (E/\rho_t)^{1/2} = 5000$ m/s and $T_{cef} = 0.3\, T_c = 0.3 * 10 = 3$ ms, so that the dynamic length scale would be 15 m. See [Lavooij & Tijsseling 1989] for the importance of timescales in FSI calculations.

The ANSI/ASME pressure piping Codes do not clearly indicate how to derive pipe stresses from dynamic pressures as calculated by classical waterhammer theory. Dynamic load factors 2 are recommended for step loads. Static stresses should be taken into account when calculating the equivalent stresses. This is usually not done in connection with a conventional waterhammer analysis.

6. Review and conclusions

The influence of the rigidity of pipe anchors on the transient behaviour of one specific reservoir-pipeline-valve system (77.5 m long 4" diameter pipeline with six bends) has been studied numerically. The anchors, located at the bends and modelled as linear springs, determine the flexibility of the pipe system. For anchors with a rigidity larger than the axial stiffness of one metre of pipe, the influence on the transient behaviour of the system is small; the classical waterhammer theory gives then reliable predictions of the pressures in the system. For less rigid anchors the motion of bends leads to severe deviations between the predictions of classical and extended waterhammer theory. Higher extreme pressures and different basic frequencies in the pressure histories are the result. Starting with a very rigid pipe system, the main frequency of the pressure wave decreases for less stiff systems until at a certain rigidity/flexibility it jumps to a higher value from which it decreases to the frequency pertaining to a system without bend supports.

For an accurate determination of the equivalent stresses in the pipe system both a static (steady-state) and a dynamic (fluid-structure interaction) stress analysis is required. With classical Joukowsky pressures as additional input in the static stress analysis only, reliable results are obtained in the more rigid pipe systems, whereas the stresses are highly underestimated in the more flexible systems.

In the more flexible systems the maximum stresses are higher, but the forces on the supports are lower.

It has been shown that a detailed analysis of the static and dynamic behaviour of liquid-filled pipe systems is possible with present-day software. Exercises like those underlying this paper might eventually lead to guidelines and design rules useful to pipe engineers.

References

Biggs J.M. 1963 *Introduction to structural dynamics*. McGraw-Hill Book Co., New York, USA.

Blade R.J., Lewis W. & Goodykoontz J.H. 1962 *Study of a sinusoidally perturbed flow in a line including a 90 degrees elbow with flexible supports*. National Aeronautics & Space Administration, Technical Note D-1216.

Bürmann W. & Thielen H. 1988 *Measurement and computation of dynamic reactive forces on pipes containing flow*. 3R international, Vol. 27, No. 6, pp. 434-440 (in German).

Chaudhry M.H. 1979 *Applied hydraulic transients*. New York: Van Nostrand Reinhold. (1st edition 1979, 2nd edition 1987)

Gere J.M. & Timoshenko S.P. 1987 *Mechanics of materials*. Van Nostrand Reinhold (UK) Co. Ltd.

Hatfield F.J., Wiggert D.C. & Otwell R.S. 1982 *Fluid structure interaction in piping by component synthesis*. ASME Journal of Fluids Engineering, Vol. 104, No. 3, pp. 318-325.

Heinsbroek A.G.T.J. 1993 *Fluid-structure interaction in non-rigid pipeline systems - comparative analyses*. ASME/TWI 12th Int. Conf. on Offshore Mechanics and Arctic Engineering, Glasgow, Scotland, UK, June 1993, Paper OMAE-93-1018, pp. 405-410.

Helguero M.V. 1985 *Piping Stress Handbook* 2nd edition. Gulf Publishing Company, Houston, USA, pp. 1-2.

Kellner A., Voss J. & Schönfelder C. 1983 *Fluid/structure-interaction in piping systems: theory and experiment*. Trans. of SMiRT7, Chicago, USA, August 1983.

Krause N., Goldsmith W. & Sackman J.L. 1977 *Transients in tubes containing liquids*. Int. Journal of Mechanical Sciences, Vol. 19, No. 1, pp. 53-68.

Kruisbrink A.C.H. & Heinsbroek A.G.T.J. 1992 *Fluid-structure interaction in non-rigid pipeline systems - large scale validation tests*. Proc. of the Int. Conf. on Pipeline Systems, BHR Group, Manchester, UK, March 1992, pp. 151-164, ISBN 0-7923-1668-1.

Lavooij C.S.W. & Tijsseling A.S. 1989 *Fluid-structure interaction in compliant piping systems*. Proc. of the 6th Int. Conf. on Pressure Surges, BHRA, Cambridge, UK, October 1989, pp. 85-100.

Simpson A.R. 1986 *Large water hammer pressures due to column separation in sloping pipes*. Ph.D. Thesis, The University of Michigan, Dep. of Civil Engineering, Ann Arbor, USA.

Skalak R. 1956 *An extension of the theory of waterhammer*. Trans. of the ASME, Vol. 78, No. 1, pp. 105-116.

Swaffield J.A. 1968-1969 *The influence of bends on fluid transients propagated in incompressible pipe flow*. Proc. of the Institution of Mechanical Engineers, Vol. 183, Part 1, No. 29, pp. 603-614.

Tijsseling A.S. & Lavooij C.S.W. 1989 *Fluid-structure interaction and column separation in a straight elastic pipe*. Proc. of the 6th Int. Conf. on Pressure Surges, BHRA, Cambridge, UK, October 1989, pp. 27-41.

Tijsseling A.S. & Lavooij C.S.W. 1990 *Waterhammer with fluid-structure interaction*. Applied Scientific Research, Vol. 47, No. 3, pp. 273-285.

Tijsseling A.S. 1993 *Fluid-structure interaction in case of waterhammer with cavitation*. Ph.D. Thesis, Delft University of Technology, Faculty of Civil Engineering, Communications on Hydraulic and Geotechnical Engineering, Report No. 93-6, ISSN 0169-6548, Delft, The Netherlands.

Vardy A.E. & Fan D. 1989 *Flexural waves in a closed tube*. Proc. of the 6th Int. Conf. on Pressure Surges, BHRA, Cambridge, UK, October 1989, pp. 43-57.

Weijde P.J. van der 1985 *Prediction of pressure surges and dynamic forces in pipeline systems, influence of system vibrations on pressures and dynamic forces (fluid structure interaction).* Symp. on Pipelines, Utrecht, The Netherlands, November 1985, The Institution of Chemical Engineers, European Branch Symposium Series 4/1985, pp. 327-335.

Wiggert D.C., Otwell R.S. & Hatfield F.J. 1985 *The effect of elbow restraint on pressure transients.* ASME Journal of Fluids Engineering, Vol. 107, No. 3, pp. 402-406.

Wiggert D.C., Hatfield F.J. & Lesmez M.W. 1986 *Coupled transient flow and structural motion in liquid-filled piping systems.* Proc. of the 5th Int. Conf. on Pressure Surges, BHRA, Hanover, Germany, September 1986, pp. 1-9.

Wilkinson D.H. 1980 *Dynamic response of pipework systems to water hammer.* Proc. of the 3rd Int. Conf. on Pressure Surges, BHRA, Canterbury, UK, March 1980, pp. 185-202.

Wood D.J. 1969 *Influence of line motion on waterhammer pressures.* ASCE Journal of the Hydraulics Division, Vol. 95, May, pp. 941-959.

Wood D.J. & Chao S.P. 1971 *Effect of pipeline junctions on water hammer surges.* ASCE Transportation Engineering Journal, Vol. 97, August, pp. 441-456.

Wylie E.B. & Streeter V.L. 1993 *Fluid transients in systems.* Englewood Cliffs, New Jersey, USA: Prentice Hall.